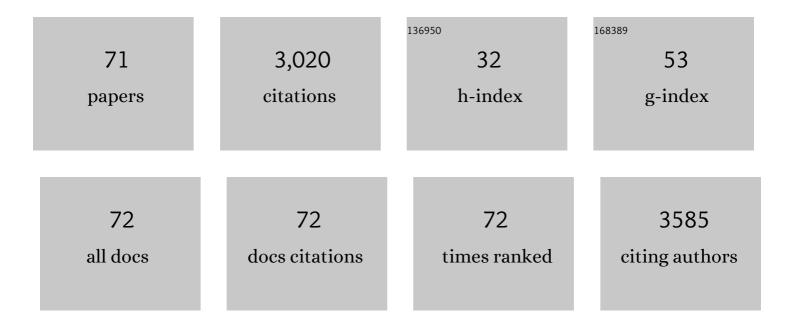
Valerie Montouillout

List of Publications by Year in descending order

Source: https://exaly.com/author-pdf/6524908/publications.pdf Version: 2024-02-01



#	Article	IF	CITATIONS
1	Nature, Structure and Strength of the Acidic Sites of Amorphous Silica Alumina:Â An IR and NMR Study. Journal of Physical Chemistry B, 2006, 110, 15172-15185.	2.6	242
2	Amorphous materials: Properties, structure, and durability: Structure of Mg- and Mg/Ca aluminosilicate glasses: 27Al NMR and Raman spectroscopy investigations. American Mineralogist, 2008, 93, 1721-1731.	1.9	187
3	Crystal structure of magnesium silicate hydrates (M-S-H): The relation with 2:1 Mg–Si phyllosilicates. Cement and Concrete Research, 2015, 73, 228-237.	11.0	139
4	Accessibility of the acid sites in dealuminated small-port mordenites studied by FTIR of co-adsorbed alkylpyridines and CO. Microporous and Mesoporous Materials, 2004, 71, 157-166.	4.4	125
5	Local Al site distribution in aluminosilicate glasses by 27Al MQMAS NMR. Journal of Non-Crystalline Solids, 2007, 353, 180-184.	3.1	121
6	Characterization of boron incorporation and speciation in calcite and aragonite from co-precipitation experiments under controlled pH, temperature and precipitation rate. Geochimica Et Cosmochimica Acta, 2015, 150, 299-313.	3.9	102
7	ODESSA, a New 1D NMR Exchange Experiment for Chemically Equivalent Nuclei in Rotating Solids. Journal of Magnetic Resonance Series A, 1996, 123, 7-15.	1.6	85
8	New Layered Calcium Organosilicate Hybrids with Covalently Linked Organic Functionalities. Chemistry of Materials, 2004, 16, 3955-3962.	6.7	82
9	Raman and 27Al NMR structure investigations of aluminate glasses: (1â^'x)Al2O3â^'x MO, with M=Ca, Sr,	3.1	82
10	of reference GaIV, GaV, and GaVI compounds by MAS and QPASS, extension of gallium/aluminum NMR parameter correlation. Solid State Nuclear Magnetic Resonance, 1999, 15, 159-169.	2.3	77
11	Synthesis, crystal structure and 71Ga solid state NMR of a MOF-type gallium trimesate (MIL-96) with μ3-oxo bridged trinuclear units and a hexagonal 18-ring network. Microporous and Mesoporous Materials, 2007, 105, 111-117.	4.4	74
12	Distribution of Water in Synthetic Calcium Silicate Hydrates. Langmuir, 2016, 32, 6794-6805.	3.5	72
13	Thermodynamic properties of C-S-H, C-A-S-H and M-S-H phases: Results from direct measurements and predictive modelling. Applied Geochemistry, 2018, 92, 140-156.	3.0	72
14	Characterization of MgAl2O4 Precursor Powders Prepared by Aqueous Route. Journal of the American Ceramic Society, 1999, 82, 3299-3304.	3.8	71
15	Order-resolved sideband separation in magic angle spinning NMR of half integer quadrupolar nuclei. Chemical Physics Letters, 1997, 272, 295-300.	2.6	60
16	Unexpected similarities between the surface chemistry of cubic and hexagonal gallia polymorphs. Physical Chemistry Chemical Physics, 2003, 5, 1301-1305.	2.8	60
17	Topological, Geometric, and Chemical Order in Materials: Insights from Solid-State NMR. Accounts of Chemical Research, 2013, 46, 1975-1984.	15.6	60
18	Structure and dynamics of oxide melts and glasses: A view from multinuclear and high temperature NMR. Journal of Non-Crystalline Solids, 2008, 354, 249-254.	3.1	59

#	Article	IF	CITATIONS
19	Detection and use of small J couplings in solid state NMR experiments. Comptes Rendus Chimie, 2010, 13, 117-129.	0.5	59
20	Double-Resonance Decoupling for Resolution Enhancement of 31P Solid-State MAS and 27Al →31 P MQHETCOR NMR. Solid State Nuclear Magnetic Resonance, 2002, 22, 501-512.	2.3	52
21	Characterisation, acidity and catalytic activity of Ga–SBA-15 materials prepared following different synthesis procedures. Applied Catalysis A: General, 2006, 309, 177-186.	4.3	52
22	The response of pre-osteoblasts and osteoclasts to gallium containing mesoporous bioactive glasses. Acta Biomaterialia, 2018, 76, 333-343.	8.3	49
23	Continuous flow hyperpolarized129Xe-MAS NMR studies of microporous materials. Physical Chemistry Chemical Physics, 2003, 5, 4479-4483.	2.8	44
24	Electrical conductivity and 11B NMR studies of sodium borosilicate glasses. Journal of Non-Crystalline Solids, 2008, 354, 1664-1670.	3.1	44
25	Synthesis and Characterization of Spinel-Type Gallia-Alumina Solid Solutions. Zeitschrift Fur Anorganische Und Allgemeine Chemie, 2005, 631, 2121-2126.	1.2	43
26	NMR and FTIR spectroscopic studies on the acidity of gallia?silica prepared by a sol?gel route. Microporous and Mesoporous Materials, 2004, 67, 259-264.	4.4	40
27	Cation Sublattice Disorder Induced by Swift Heavy Ions in MgAl ₂ O ₄ and ZnAl ₂ O ₄ Spinels: ²⁷ Al Solid-State NMR Study. Journal of Physical Chemistry B, 2007, 111, 12707-12714.	2.6	38
28	Structural fluctuations and role of Ti as nucleating agent in an aluminosilicate glass. Journal of Non-Crystalline Solids, 2010, 356, 1368-1373.	3.1	37
29	Resolution enhancement in solid-state MQ-MAS experiments achieved by composite decoupling. Magnetic Resonance in Chemistry, 1998, 36, 956-959.	1.9	36
30	1D to 3D NMR study of microporous aluminoâ€phosphate AlPO ₄ â€40. Magnetic Resonance in Chemistry, 2009, 47, 942-947.	1.9	36
31	Bioactive glass–gelatin hybrids: building scaffolds with enhanced calcium incorporation and controlled porosity for bone regeneration. Journal of Materials Chemistry B, 2016, 4, 2486-2497.	5.8	34
32	Study of the alkaline environment in mixed alkali compositions by multiple-quantum magic angle nuclear magnetic resonance (MQ–MAS NMR). Journal of Non-Crystalline Solids, 2008, 354, 333-340.	3.1	33
33	Theoretical isotopic fractionation between structural boron in carbonates and aqueous boric acid and borate ion. Geochimica Et Cosmochimica Acta, 2018, 222, 117-129.	3.9	33
34	Synthesis and Structure Resolution of RbLaF4. Inorganic Chemistry, 2012, 51, 2272-2282.	4.0	32
35	Synthesis and Structure Determination of CaSi _{1/3} B _{2/3} O _{8/3} : A New Calcium Borosilicate. Inorganic Chemistry, 2013, 52, 4250-4258.	4.0	31
36	Experimental constraints on Li isotope fractionation during the interaction between kaolinite and seawater. Geochimica Et Cosmochimica Acta, 2021, 292, 333-347.	3.9	30

#	Article	IF	CITATIONS
37	Ionic conductivity of lithium borate glasses and local structure probed by high resolution solid-sate NMR. Journal of Non-Crystalline Solids, 2018, 484, 57-64.	3.1	29
38	Hydration Properties and Interlayer Organization in Synthetic C-S-H. Langmuir, 2020, 36, 9449-9464.	3.5	28
39	Through-bond homonuclear correlation experiments in solid-state NMR applied to quadrupolar nuclei in Al–O–P–O–Al chains. Chemical Communications, 2006, , 1924-1925.	4.1	26
40	Alkylation of thiophenic compounds over heteropoly acid H3PW12O40 supported on MgF2. Applied Catalysis B: Environmental, 2014, 152-153, 241-249.	20.2	25
41	Chemical durability of peraluminous glasses for nuclear waste conditioning. Npj Materials Degradation, 2018, 2, .	5.8	25
42	Mechanism of Calcium Incorporation Inside Sol–Gel Silicate Bioactive Glass and the Advantage of Using Ca(OH) ₂ over Other Calcium Sources. ACS Biomaterials Science and Engineering, 2019, 5, 5906-5915.	5.2	25
43	Evidence for Discrepancy between the Surface Lewis Acid Site Strength and Infrared Spectra of Adsorbed Molecules:Â The Case of Boriaâ°'Silica. Journal of Physical Chemistry B, 2004, 108, 16499-16507.	2.6	24
44	Structural evolution of high zirconia aluminosilicate glasses. Journal of Non-Crystalline Solids, 2020, 539, 120050.	3.1	23
45	A one step process for grafting organic pendants on alumina via the reaction of alumina and phosphonate under microwave irradiation. Chemical Communications, 2001, , 2060-2061.	4.1	22
46	Toward a better description of gallo-phosphate materials in solid-state NMR: 1D and 2D correlation studies. Magnetic Resonance in Chemistry, 2006, 44, 770-775.	1.9	22
47	Environment of titanium and aluminum in a magnesium alumino-silicate glass. Journal of Physics Condensed Matter, 2009, 21, 375107.	1.8	22
48	Homogeneity of peraluminous SiO 2 –B 2 O 3 –Al 2 O 3 –Na 2 O–CaO–Nd 2 O 3 glasses: Effect of neodymium content. Journal of Non-Crystalline Solids, 2014, 405, 55-62.	3.1	21
49	High catalytic cracking activity of Al-MCM-41 type materials prepared from ZSM-5 zeolite crystals and fumed silica. Applied Catalysis A: General, 2008, 344, 61-69.	4.3	20
50	Deconvolution method of 29Si MAS NMR spectra applied to homogeneous and phase separated lanthanum aluminosilicate glasses. Journal of Non-Crystalline Solids, 2019, 503-504, 352-365.	3.1	18
51	Biosourced analogs of elastomer-containing bitumen through hydrothermal liquefaction of Spirulina sp. microalgae residues. Green Chemistry, 2018, 20, 2337-2344.	9.0	17
52	Bioactive glass hybrids: a simple route towards the gelatin–SiO ₂ –CaO system. Chemical Communications, 2014, 50, 8701.	4.1	16
53	A straightforward approach to enhance the textural, mechanical and biological properties of injectable calcium phosphate apatitic cements (CPCs): CPC/blood composites, a comprehensive study. Acta Biomaterialia, 2017, 62, 328-339.	8.3	15
54	Assembly of benzene-1,3,5-tris(methylenephosphonic acid) and guanidinium salt: Single crystal-X-ray characterisation and31P solid state NMR investigations. New Journal of Chemistry, 2004, 28, 1244-1249.	2.8	13

VALERIE MONTOUILLOUT

#	Article	IF	CITATIONS
55	Rearrangement of the structure during nucleation of a cordierite glass doped with TiO ₂ . Journal of Physics Condensed Matter, 2010, 22, 185401.	1.8	13
56	Effect of composition on peraluminous glass properties: An application to HLW containment. Journal of Nuclear Materials, 2017, 483, 90-101.	2.7	12
57	Quantitative mineralogical mapping of hydrated low pH concrete. Cement and Concrete Composites, 2017, 83, 360-373.	10.7	12
58	Ionic conductivity and boron anomaly in binary lithium borate melts. Journal of Non-Crystalline Solids, 2020, 543, 120160.	3.1	12
59	Self-Association Of Benzene-1,3,5-Tris-(Methylenephosphonic Acid): Evidence of Charge-Assisted Hydrogen Bonds. Molecular Crystals and Liquid Crystals, 2002, 389, 87-95.	0.9	11
60	Design and properties of a novel radiopaque injectable apatitic calcium phosphate cement, suitable for imageâ€guided implantation. Journal of Biomedical Materials Research - Part B Applied Biomaterials, 2018, 106, 2786-2795.	3.4	11
61	Identification of tetrahedrally ordered Si–O–Al environments in molecular sieves by {27Al}–29Si REAPDOR NMR. Chemical Physics Letters, 2004, 390, 79-83.	2.6	10
62	Vitrification, crystallization behavior and structure of zinc aluminosilicate glasses. Journal of Non-Crystalline Solids, 2021, 555, 120609.	3.1	10
63	Glass structure of industrial ground granulated blast furnace slags (CGBS) investigated by time-resolved Raman and NMR spectroscopies. Journal of Materials Science, 2021, 56, 17490-17504.	3.7	8
64	Palladium complex immobilised on zirconium-phosphite: characterisation by 31P MAS NMR and TEM and behaviour towards reducing agents. Journal of Molecular Structure, 2003, 659, 135-142.	3.6	7
65	Direct evidence of the role of dispersed ceria on the activation of oxygen in NaX zeolite by coupling the 170/160 isotopic exchange and 170 solid-state NMR. Journal of Catalysis, 2013, 300, 136-140.	6.2	7
66	Towards higher resolution for quadrupolar nuclei in solid state NMR at very high field. Comptes Rendus De L'Academie Des Sciences - Series IIc: Chemistry, 1998, 1, 157-162.	0.1	6
67	Impact of trace metals Zn, Cu, Cd and Ni on the reactivity of OPC and GGBS-based hydraulic binders at early age for sediment stabilization. Construction and Building Materials, 2022, 346, 128406.	7.2	5
68	QPASS: towards higher resolution in NMR of half integer quadrupolar nuclei with high quadrupolar couplings. Journal De Chimie Physique Et De Physico-Chimie Biologique, 1998, 95, 270-279.	0.2	4
69	Study of alkaline metal ions and glass-formers in glasses with advanced NMR methods and quantum mechanic calculations. Journal of Non-Crystalline Solids, 2010, 356, 187-200.	3.1	3
70	Thermodynamic properties of mixed-layer illite-smectite by calorimetric methods: Acquisition of the enthalpies of mixing of illite and smectite layers. Journal of Chemical Thermodynamics, 2019, 138, 78-97.	2.0	3
71	Titanium in GGBS-like calcium-magnesium-aluminosilicate glasses: Its role in the glass network, dissolution at alkaline pH and surface layer formation. Journal of Non-Crystalline Solids, 2022, 591, 121708.	3.1	2